Downloaded from jnm.snmjournals.org by on March 14, 2017. For personal use only.

Comparison of [^{18}F]FDG PET and ^{201}Tl SPECT in Evaluation of Pulmonary Nodules

Kotaro Higashi, Yoshimichi Ueda, Tsutomu Sakuma, Hiroyasu Seki, Manabu Oguchi, Mitsuru Taniguchi, Suzuka Taki, Hisao Tonami, Shogo Katsuda, and Itaru Yamamoto

Departments of Radiology, Pathology, and Thoracic Surgery, Kanazawa Medical University, Kanazawa; and Department of Radiology, Kanazawa Cardiovascular Hospital, Kanazawa, Japan

Recent reports have indicated the value of [^{18}F]FDG PET and ^{201}Tl SPECT in diagnosing lung cancer. In this study, we compared the diagnostic value of FDG PET and ^{201}Tl SPECT in the evaluation of pulmonary nodules. **Methods:** Sixty-three patients with 66 pulmonary nodules suspected to be lung cancer on the basis of chest CT were examined by FDG PET and ^{201}Tl SPECT (early and delayed scans) within a week of each study. For semiquantitative analysis, the standardized uptake value (SUV) or the tumor-to-nontumor activity ratio (T/N) (or both) was calculated. All of these lesions were completely removed thoracoscopically or by thoracotomy and were examined histologically. **Results:** Fifty-four nodules were histologically confirmed to be malignant tumors, and 12 were benign. Both techniques delineated focal lesions with an increase in tracer accumulation in 41 of 54 lung cancers. ^{201}Tl SPECT on early or delayed scans (or both) identified 4 additional lung cancers that FDG PET images did not reveal: 3 bronchioloalveolar carcinomas and a well-differentiated adenocarcinoma. FDG PET identified 3 additional lung cancers that ^{201}Tl SPECT images did not reveal; 2 of these lung cancers were $<$2 cm in diameter. The mean FDG SUV and T/N of bronchioloalveolar carcinomas (2.06 $\pm$ 0.76 and 3.49 $\pm$ 1.03, respectively) were significantly lower than those of poorly differentiated adenocarcinomas (5.55 $\pm$ 2.01 [$P = 0.026$] and 8.23 $\pm$ 2.16 [$P = 0.01$], respectively). However, no significant difference was found in ^{201}Tl T/N on early and delayed scans between bronchioloalveolar carcinomas (1.64 $\pm$ 0.29 and 1.87 $\pm$ 0.42, respectively) and poorly differentiated adenocarcinomas (1.58 $\pm$ 0.32 and 2.76 $\pm$ 1.36, respectively). Of the 12 benign nodules, FDG PET and ^{201}Tl SPECT showed false-positive results for the same 7 benign nodules (58.3%) (4 granulomas, 1 sarcoidosis, 1 inflammatory pseudotumor, and 1 aspergilloma). Negative FDG PET findings and positive ^{201}Tl SPECT findings were obtained only for bronchioloalveolar carcinomas or a well-differentiated adenocarcinoma but not for other histologic types of lung cancers or benign pulmonary nodules. **Conclusion:** No significant difference was found between FDG PET and ^{201}Tl SPECT in specificity for the differentiation of malignant and benign pulmonary nodules. The degree of differentiation of lung adenocarcinoma correlated with FDG uptake but not with ^{201}Tl uptake. Bronchioloalveolar carcinoma (a well-differentiated, slow-growing tumor) findings typically were positive with ^{201}Tl but were negative with FDG. The combination of FDG PET and ^{201}Tl SPECT may provide additional information regarding the tissue characterization of pulmonary nodules.

Key Words: PET; lung cancer; ^{201}Tl; [^{18}F]FDG

J Nucl Med 2001; 42:1489–1496

Chest radiography and CT are frequently performed on patients with suspected lung cancer. These modalities provide anatomic and morphologic information, but they do not accurately characterize abnormalities as benign or malignant. The diagnosis has required tissue obtained by sputum cytology or biopsy. More than 50% of radiographically indeterminate lesions resected by thoracoscopy are benign (*1*).

Recent reports have indicated the value of [^{18}F]FDG PET and ^{201}Tl SPECT in diagnosing lung cancer. Several recent studies have shown that PET with FDG is accurate in differentiating between benign and malignant pulmonary lesions (*2–4*). FDG PET has a sensitivity and a specificity of 98% and 69%, respectively, for detecting malignancy in indeterminate solitary pulmonary nodules (*2*). ^{201}T1 accumulation on SPECT also differs between benign and malignant tumors (*5–7*). ^{201}Tl accumulations are seen in malignant tumors on early and delayed scans but not on the delayed scan of benign tumors. Retention of ^{201}Tl on delayed scans is strongly suggestive of malignancy (*5–7*).

However, on closer inspection of the literature, strong FDG uptake can be seen in a variety of inflammatory lesions (*2,8–13*). In particular, the degree and type of inflammatory responses are important in determining FDG uptake. Tuberculosis, sarcoidosis, inflammatory pseudotumor, fungal infection, pneumonia, and abscess have all been associated with FDG uptake (*2,9,12,13*). These infections are characterized by cellular infiltrates, granuloma formation, and macrophage proliferation. ^{201}Tl is also absorbed into the inflammatory lesions (*14*) and has been reported to be of value in the evaluation of disease activity (*15*).

FDG PET remains an expensive and complicated procedure, which is performed with tracers and imaging equipment that are available at a limited number of sites. In contrast, the technology needed to perform lung SPECT

Received Oct. 12, 2000; revision accepted Apr. 9, 2001.

For correspondence or reprints contact: Kotaro Higashi, MD, Department of Radiology, Kanazawa Medical University, 1-1, Uchinada, Daigaku, Kahoku-gun, Ishikawa, 920-0293, Japan.

Downloaded from jnm.snmjournals.org by on March 14, 2017. For personal use only.

with ^{201}Tl is widely available at only a fraction of the cost of PET. Furthermore, FDG PET may show negative results for bronchioloalveolar carcinoma (*16*). In a previous comparison of the diagnostic value of FDG PET imaging and ^{201}Tl SPECT imaging in the detection of lung cancer (*17*) we concluded that the sensitivity of ^{201}Tl SPECT is comparable with that of FDG PET in the detection of lung cancers > 2 cm in diameter. However, the study included only a few cases of bronchioloalveolar carcinoma; thus, the detection sensitivity for bronchioloalveolar carcinomas was not compared between FDG PET and ^{201}Tl SPECT. Furthermore, the study included only cases of histologically proven lung cancer. Therefore, the specificity in differentiating malignant and benign pulmonary nodules was also not compared between FDG PET and ^{201}Tl SPECT. For these reasons, we performed a comparison of the 2 scintigraphic examinations in patients with pulmonary nodules to estimate the value of these modalities in the detection of bronchioloalveolar carcinoma and their specificity in differentiating malignant and benign pulmonary nodules.

MATERIALS AND METHODS

Patients

This study included 63 patients (29 men, 34 women; age range, 42–85 y; mean age, 65 y) with 66 pulmonary nodules suspected to be lung cancer on the basis of chest CT who had undergone preoperative FDG PET and ^{201}Tl SPECT between February 1994 and August 1999. Double pulmonary nodules were observed in 3 patients. FDG PET and ^{201}Tl SPECT studies were completed within a week of each other, and all patients underwent thoracotomy, open lung biopsy, or lung biopsy using video-assisted thoracoscopic surgery in the 4 wk after their FDG and ^{201}Tl studies. All of these lesions were removed completely and were examined histologically. None of the patients had insulin-dependent diabetes, and serum glucose levels just before the injection of FDG were <120 mg/dL in all patients. Informed consent was obtained from patients participating in the study.

FDG PET

PET was performed using a dedicated PET camera (Headtome IV; Shimazu, Kyoto, Japan) with 4 rings, which provided 7 tomographic slices. The intrinsic resolution was 5 mm full width at half maximum at the center. After at least 4 h of fasting, each subject underwent transmission scanning for attenuation correction for 10 min. Immediately after obtaining the transmission scan, FDG were administered intravenously, and a static scan (14–24 tomographic slices at 6.5-mm intervals) was obtained 40 min later for 10–20 min using a 128 × 128 matrix. The average injection dose of FDG was 185 MBq.

^{201}Tl SPECT

All patients were examined with ^{201}Tl SPECT within a week of the PET study. With the subjects at rest, 111 MBq ^{201}Tl-chloride were injected into a peripheral vein, and ^{201}Tl imaging was begun 15 min (early scan) and 3 h (delayed scan) later. SPECT was performed using a triple-head rotating gamma camera system (PRISM 3000; Picker International, Cleveland, OH) equipped with a high-resolution collimator; 30 projection images were collected for 40 s each over 360° using a 128 × 128 matrix. The total acquisition time was approximately 30 min. The intrinsic resolution was 15 mm full width at half maximum at the center. The slice thickness was 5.8 mm. A series of transverse slices was reconstructed with filtered backprojection using a ramp Hanning filter with a cutoff frequency of 0.5 cycle/pixel. No attenuation correction was performed.

Data Analysis

The FDG and ^{201}Tl images were interpreted visually from the films and correlated carefully with the CT study at the same time. For qualitative analysis, any obvious foci of increased FDG or ^{201}Tl uptake over background were considered positive for tumor. For semiquantitative analysis of the FDG uptake, regions of interest (ROIs) were defined manually on the transaxial tomograms that showed the lesion's highest uptake to be the middle of the tumor. The ROIs placed on the lesions encompassed all pixels that had uptake values of >90% of the maximum uptake in that slice, and the average counting rate in each ROI was calculated. After correction for radioactive decay, the ROIs were analyzed by computing the standardized uptake value ([SUV] tumor activity concentration/injected dose/body weight). The SUVs were calculated using a calibration factor between PET counts and radioactivity concentration. No recovery coefficient correction was applied. Tumor-to-nontumor activity ratios (T/Ns) were also calculated between the lesions and the homologous contralateral normal lung. For semiquantitative analysis of ^{201}Tl SPECT, ROIs were defined manually on the transaxial tomograms that showed the lesion's highest uptake to be the middle of the tumor. The ROIs placed on the lesions encompassed all pixels that had uptake values of >90% of the maximum uptake in that slice, and the average counting rate in each ROI was calculated. The radioactivity was also measured for areas of the homologous contralateral normal lung to calculate the T/N of the activity on early scans (early ratio [ER]) and on delayed scans (delayed ratio [DR]). The retention index (RI) of ^{201}Tl was also calculated for tumor activity according to the following equation: retention index (%) = (DR − ER) × 100/ER.

Statistical Analysis

The comparison of differences in FDG and ^{201}Tl uptake was performed using the 2-tailed Student *t* test for unpaired data. $P < 0.05$ were considered to be statistically significant.

RESULTS

Fifty-four nodules were histologically confirmed malignant tumors, and 12 were histologically confirmed benign nodules (Tables 1 and 2). The 54 malignant nodules consisted of 44 adenocarcinomas, including 11 bronchioloalveolar carcinomas, 6 squamous cell carcinomas, 2 adenosquamous cell carcinomas, 1 large cell carcinoma, and 1 metastatic lung cancer. Twelve benign nodules consisted of 4 granulomas, 3 pulmonary infarctions associated with dirofilariasis, 1 chronic inflammatory change, 1 aspergilloma, 1 abscess, 1 inflammatory pseudotumor, and 1 sarcoidosis. The size of the pulmonary nodules was determined from the resected specimens and ranged from 0.8 to 6.3 cm. Twenty-two of the pulmonary nodules (33.3%) were >3 cm in diameter. Of the remaining 44 nodules, 19 (28.8%) were 2.0–2.9 cm, and 25 (37.9%) were <1.9 cm. Tables 1 and 2 summarize the results of the radionuclide and pathologic findings for the 66 pulmonary nodules studied.

Downloaded from jnm.snmjournals.org by on March 14, 2017. For personal use only.

TABLE 1
Patients' Characteristics and Radionuclide Imaging Results: Malignant Nodules

Patient no.	Age (y)	Sex	Histologic type	Size (cm)	FDG		^{201}Tl		
					SUV	T/N	ER	DR	RI (%)
1	70	F	BAC	1.2	Neg.	Neg.	Neg.	Neg.	NA
2	51	F	BAC	1.2	Neg.	Neg.	Neg.	Neg.	NA
3*	76	F	BAC	1.7	1.27	2.33	1.30	Neg.	NA
4	69	F	BAC	1.9	Neg.	Neg.	1.75	Neg.	NA
5	78	F	BAC	2.0	Neg.	Neg.	Neg.	1.56	NA
6	76	F	BAC	2.0	Neg.	Neg.	1.39	1.79	28.8
7	54	F	BAC	2.2	Neg.	Neg.	Neg.	Neg.	NA
8	49	F	BAC	2.5	Neg.	Neg.	Neg.	Neg.	NA
9	50	F	BAC	2.6	Neg.	Neg.	Neg.	Neg.	NA
10	63	F	BAC	3.8	2.78	3.86	1.97	2.48	25.9
11	67	M	BAC	4.0	2.14	4.29	1.81	1.64	−9.4
12†	68	M	Well-diff. AC	1.4	3.86	5.82	1.51	2.59	71.5
13	51	M	Well-diff. AC	1.7	2.03	3.19	1.35	Neg.	NA
14	81	F	Well-diff. AC	1.8	4.52	5.47	1.74	1.83	5.2
15	46	F	Well-diff. AC	1.9	2.32	1.97	Neg.	1.53	NA
16	48	F	Well-diff. AC	2.0	1.78	2.66	1.84	2.20	19.6
17	62	F	Well-diff. AC	2.0	1.24	3.13	1.56	1.56	0
18	49	M	Well-diff. AC	2.4	Neg.	Neg.	1.50	2.62	74.7
19	64	F	Well-diff. AC	3.0	3.25	8.95	2.10	3.02	43.8
20	67	F	Well-diff. AC	3.1	3.71	8.40	1.69	4.02	137.9
21	70	M	Well-diff. AC	3.2	4.41	10.80	2.43	3.81	56.8
22	79	F	Well-diff. AC	4.5	4.48	7.16	2.41	3.60	49.4
23	75	M	Well- to mod. diff. AC	1.8	2.52	2.04	Neg.	1.68	NA
24	65	M	Well- to mod. diff. AC	2.8	1.79	5.39	3.09	3.47	12.3
25†	68	M	Mod. diff. AC	1.1	2.00	2.17	1.59	Neg.	NA
26	42	F	Mod. diff. AC	1.5	2.64	3.59	Neg.	Neg.	NA
27	47	F	Mod. diff. AC	1.6	2.04	2.46	Neg.	1.83	NA
28	63	M	Mod. diff. AC	1.8	3.81	5.14	Neg.	Neg.	NA
29*	76	F	Mod. diff. AC	1.9	3.76	10.70	1.70	1.63	−4.1
30	72	F	Mod. diff. AC	2.0	1.79	3.75	1.31	1.55	18.3
31	53	F	Mod. diff. AC	2.5	5.31	6.17	1.44	2.18	51.4
32	73	M	Mod. diff. AC	2.8	2.35	4.01	Neg.	1.86	NA
33	53	M	Mod. diff. AC	2.9	5.76	6.60	1.36	2.09	53.7
34	59	F	Mod. diff. AC	3.5	2.12	3.72	1.23	2.32	88.6
35	59	F	Mod. diff. AC	3.5	7.06	8.26	Neg.	Neg.	NA
36	64	M	Mod. diff. AC	3.6	5.94	16.80	2.46	2.97	20.7
37	68	M	Mod. diff. AC	3.8	4.87	9.44	2.21	2.45	10.9
38	75	M	Mod. diff. AC	4.9	6.05	12.80	3.86	4.24	9.8
39	85	M	Poorly diff. AC	0.8	2.11	6.65	1.90	3.87	103.7
40	71	M	Poorly diff. AC	2.5	6.13	5.01	1.44	2.45	70.1
41‡	50	M	Poorly diff. AC	3.2	5.80	10.58	1.17	Neg.	NA
42	54	M	Poorly diff. AC	4.0	8.29	7.78	1.83	4.48	144.8
43‡	50	M	Poorly diff. AC	5.2	5.02	9.17	1.84	1.55	−15.8
44	59	M	Poorly diff. AC	5.5	5.97	10.20	1.28	1.47	14.8
45	66	M	SCC	1.5	4.77	4.95	Neg.	1.71	NA
46	75	M	SCC	1.7	3.72	5.05	2.27	2.82	24.2
47	71	M	SCC	2.0	5.30	23.80	2.66	3.31	24.4
48	76	M	SCC	3.0	7.22	12.90	2.91	4.79	64.6
49	64	M	SCC	4.0	6.19	8.96	1.44	1.92	33.3
50	70	M	SCC	6.3	9.74	29.80	3.83	3.54	−7.6
51	73	M	Adeno-SCC	2.7	9.86	16.10	3.37	3.26	−3.3
52	76	M	Adeno-SCC	3.1	7.90	8.21	1.78	2.42	36.0
53	82	F	Large cell carcinoma	1.8	3.26	6.16	1.72	2.42	40.7
54	67	F	Metastatic lung carcinoma	1.5	Neg.	Neg.	Neg.	Neg.	NA

*Same patient.
†Same patient.
‡Same patient.
BAC = bronchioloalveolar carcinoma; Neg. = negative; NA = not applicable; diff. = differentiated; AC = adenocarcinoma; mod. or Mod. = moderately; SCC = squamous cell carcinoma; Adeno-SCC = adenosquamous cell carcinoma.

Downloaded from jnm.snmjournals.org by on March 14, 2017. For personal use only.

TABLE 2
Patients' Characteristics and Radionuclide Imaging Results: Benign Nodules

Patient no.	Age (y)	Sex	Histologic type	Size (cm)	FDG		^{201}Tl		
					SUV	T/N	ER	DR	RI (%)
55	60	F	Epitheroid granuloma	1.0	1.48	3.55	1.62	Neg.	NA
56	69	F	Dirofilariasis	1.2	Neg.	Neg.	Neg.	Neg.	NA
57	60	F	Chronic inflammatory change	1.4	Neg.	Neg.	Neg.	Neg.	NA
58	55	M	Aspergilloma	1.5	1.82	2.46	2.26	Neg.	NA
59	74	F	Epitheroid granuloma	1.5	3.48	6.86	1.58	1.65	4.4
60	47	M	Necrotizing granuloma	2.0	1.25	5.94	Neg.	1.22	NA
61	67	F	Abscess	2.2	Neg.	Neg.	Neg.	Neg.	NA
62	51	F	Necrotizing granuloma	2.2	4.53	3.87	Neg.	2.13	NA
63	58	M	Dirofilariasis	2.5	Neg.	Neg.	Neg.	Neg.	NA
64	44	F	Inflammatory pseudotumor	3.0	1.99	3.54	1.83	2.01	9.8
65	79	F	Dirofilariasis	3.0	Neg.	Neg.	Neg.	Neg.	NA
66	81	F	Sarcoidosis	3.1	10.3	15.30	1.63	2.33	42.9

Neg. = negative; NA = not applicable.

Visual Analysis

Both techniques delineated focal lesions with an increase in tracer accumulation in 41 of 54 lung cancers (Table 3). ^{201}Tl SPECT on early or delayed scans (or both) identified 4 additional lung cancers that FDG PET images did not reveal (Table 3). Three of these lung cancers were bronchioloalveolar carcinomas (patients 4–6). Another lung cancer was a well-differentiated adenocarcinoma (patient 17). Thus, bronchioloalveolar carcinoma and well-differentiated adenocarcinoma may be revealed only on ^{201}Tl SPECT but not on FDG PET. A representative case is shown in Figure 1. FDG PET identified 3 additional lung cancers that ^{201}Tl SPECT images did not reveal (Table 3). Two of these lung cancers were moderately differentiated adenocarcinomas < 2 cm in diameter (patients 26 and 28). A representative case is shown in Figure 2. Another lung cancer was a moderately differentiated adenocarcinoma that was 3.5 cm in size and was localized near a normal distribution of thallium in the myocardium (patient 35). Neither FDG PET nor ^{201}Tl SPECT revealed any lesions in 6 lung cancers (Table 3). Five of these lung cancers were bronchioloalveolar carcinomas (patients 1, 2, and 7–9). Another lung cancer was a metastatic lung cancer with necrosis (patient 54).

In the detection of lung cancer, except for bronchioloalveolar carcinoma, FDG PET (41/43 [95.3%]) provided higher sensitivity than did ^{201}Tl SPECT (39/43 [90.7%]). In contrast, in the detection of bronchioloalveolar carcinoma, ^{201}Tl SPECT (6/11 [54.5%]) provided higher sensitivity than did FDG PET (3/11 [27.3%]), although these differences were not statistically significant.

Of the 12 benign nodules, FDG PET and ^{201}Tl SPECT showed false-positive results for the same 7 benign nodules (58.3%) (4 granulomas, 1 sarcoidosis, 1 inflammatory pseudotumor, and 1 aspergilloma) (Table 2). A representa-

TABLE 3
Comparison of FDG PET and ^{201}Tl SPECT in Detection of 54 Lung Cancers

^{201}Tl SPECT	FDG PET	
	+	−
+	41	4*
−	3†	6

*Three bronchioloalveolar carcinomas and 1 well-differentiated adenocarcinoma.

†Two moderately differentiated adenocarcinomas <2 cm in size and 1 moderately differentiated adenocarcinoma localized near a normal distribution of ^{201}Tl in myocardium.

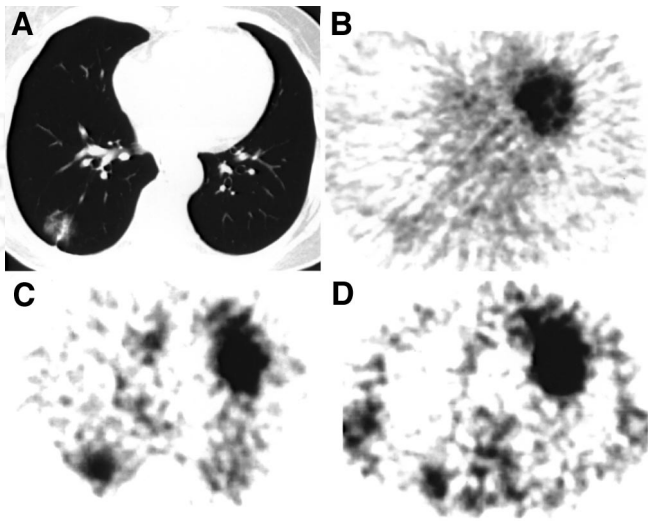

FIGURE 1. Patient 6 with bronchioloalveolar adenocarcinoma (2.0 × 2.0 cm), pT1N0M0. (A) CT image shows nodule in right lung. (B) FDG PET image does not reveal any lesions. (C) Early scan on ^{201}Tl SPECT. (D) Delayed scan on ^{201}Tl SPECT. ^{201}Tl SPECT reveals good visualization of tumor (ER, 1.39; DR, 1.79; RI, 28.8%).

Downloaded from jnm.snmjournals.org by on March 14, 2017. For personal use only.

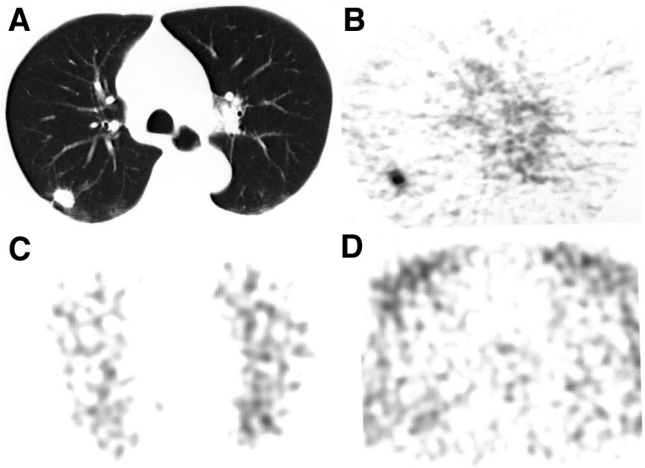

FIGURE 2. Patient 28 with moderately differentiated adenocarcinoma (1.8 × 1.2 cm), pT1N0M0. (A) CT image shows nodule in right lung. (B) FDG PET image shows hot accumulation in tumor (SUV, 3.81; T/N, 5.14). (C) Early scan on ^{201}Tl SPECT. (D) Delayed scan on ^{201}Tl SPECT. Neither early nor delayed ^{201}Tl SPECT revealed any lesions.

tive case is shown in Figure 3 (patient 66). No significant difference was found in the specificity between FDG PET and ^{201}Tl SPECT for differentiating malignant and benign pulmonary nodules. In the evaluation of pulmonary nodules using FDG PET and ^{201}Tl SPECT, negative FDG PET findings and positive ^{201}Tl SPECT findings were observed only for bronchioloalveolar carcinomas or a well-differentiated adenocarcinoma but not for other histologic types of lung cancers or benign pulmonary lesions.

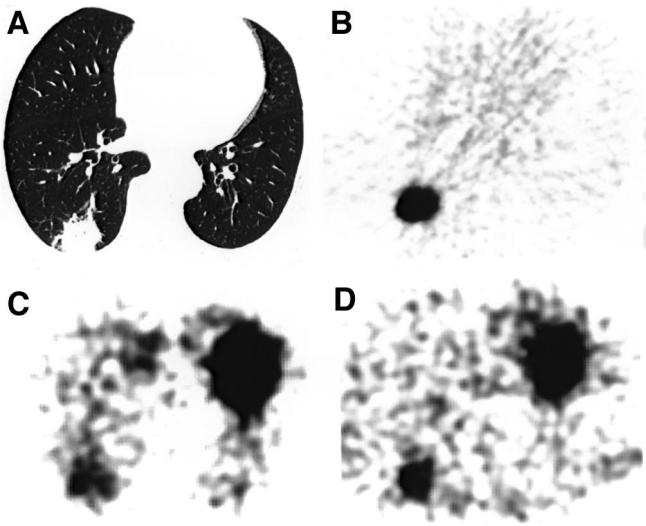

FIGURE 3. Patient 66 with sarcoidosis (3.1 × 2.7 cm). (A) CT image shows nodule in right lung. (B) FDG PET image shows hot accumulation in nodule (SUV, 10.3; T/N, 15.3). (C) Early scan on ^{201}Tl SPECT. (D) Delayed scan on ^{201}Tl SPECT. ^{201}Tl SPECT reveals good visualization of nodule (ER, 1.63; DR, 2.33; RI, 42.9%).

Semiquantitative Analysis

Among the patients showing increased tracer accumulation, the mean FDG SUV and T/N of lung cancers (4.23 ± 2.25 and 7.64 ± 5.61, respectively) were higher than those of benign nodules (3.55 ± 3.20 and 5.93 ± 4.40, respectively). The mean ^{201}Tl ER, DR, and RI of lung cancers (1.95 ± 0.69, 2.56 ± 0.93, and 38.11% ± 39.32%, respectively) were also higher than those of benign nodules (1.78 ± 0.28, 1.87 ± 0.44, and 19.03% ± 20.85%, respectively). However, these differences were not statistically significant. In benign nodules, sarcoidosis showed a markedly elevated SUV of approximately 10 (patient 66) (Fig. 3). The ^{201}Tl RI for sarcoidosis was also high (42.9%).

The mean FDG SUV and T/N of bronchioloalveolar carcinomas (2.06 ± 0.76 and 3.49 ± 1.03, respectively) were significantly lower than those of poorly differentiated adenocarcinomas (5.55 ± 2.01 [$P = 0.026$] and 8.23 ± 2.16 [$P = 0.01$], respectively) (Fig. 4), whereas no significant difference in average size was apparent between these histologic types (bronchioloalveolar carcinomas, 2.28 ± 0.92 cm; poorly differentiated adenocarcinomas, 3.53 ± 1.76 cm). Thus, a correlation was seen between FDG uptake and the degree of cell differentiation in adenocarcinoma of the lung. However, in ^{201}Tl ER, DR, and RI, no significant difference was found between bronchioloalveolar carcinomas (1.64 ± 0.29, 1.87 ± 0.42, and 15.1% ± 21.3%, respectively) and poorly differentiated adenocarcinomas (1.58 ± 0.32, 2.76 ± 1.36, and 63.5% ± 65.1%, respec-

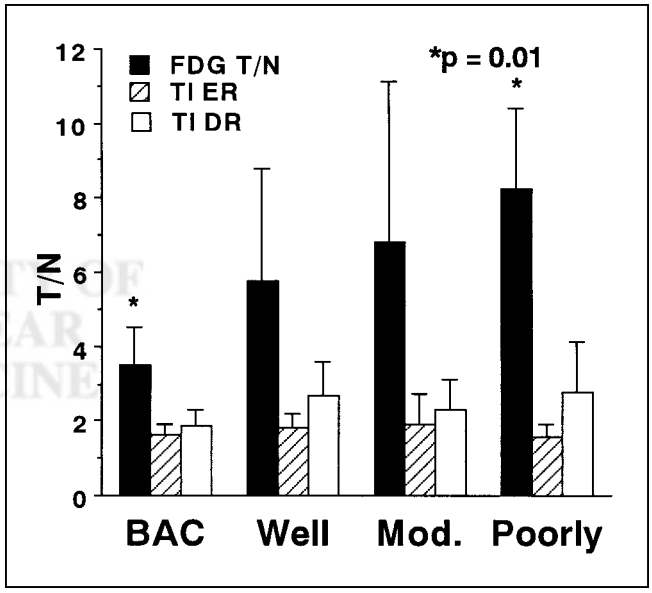

FIGURE 4. Correlation was seen between FDG T/N and degree of cell differentiation in adenocarcinoma of lung. However, in ^{201}Tl ER and DR, no significant difference was found between bronchioloalveolar carcinomas and poorly differentiated adenocarcinomas. In lung adenocarcinoma, FDG uptake, but not ^{201}Tl uptake, reflects degree of cell differentiation. BAC = bronchioloalveolar carcinoma; Well = well-differentiated adenocarcinoma; Mod. = moderately differentiated adenocarcinoma; Poorly = poorly differentiated adenocarcinoma.

Downloaded from jnm.snmjournals.org by on March 14, 2017. For personal use only.

tively) (Fig. 4). Thus, FDG uptake, not ^{201}Tl uptake, reflects the degree of cell differentiation in lung adenocarcinoma.

DISCUSSION

Our principal finding in this study was that ^{201}Tl SPECT identified 3 bronchioloalveolar carcinomas and a well-differentiated adenocarcinoma, none of which was revealed by FDG PET. Thus, bronchioloalveolar carcinoma and well-differentiated adenocarcinoma may be visualized only on ^{201}Tl SPECT but not on FDG PET. This phenomenon is explained by the finding that FDG uptake, not ^{201}Tl uptake, reflects the degree of cell differentiation in lung adenocarcinoma. The uptake of FDG by adenocarcinomas correlates with their degree of cell differentiation, and the increased FDG uptake correlates with the lesser differentiation of adenocarcinoma (*16*). Glut-1 glucose transporter expression and FDG uptake correlate with the degree of cell differentiation in adenocarcinomas, and Glut-1 expression and FDG uptake are significantly lower in bronchioloalveolar carcinomas than in nonbronchioloalveolar carcinomas (*18*). FDG uptake is related to the proliferation potential of lung cancer as estimated by the proliferating cell nuclear antigen labeling index (*19*) as well as by the doubling time (*20*), and the proliferative potential of bronchioloalveolar carcinomas is lower than that of nonbronchioloalveolar carcinomas (*19*). Regarding the relationship between ^{201}Tl uptake and cell differentiation in lung cancer, the ^{201}Tl T/N (delayed ratio) for well-differentiated adenocarcinomas is lower than that for moderately and poorly differentiated adenocarcinomas (*21*). However, intense and prolonged ^{201}Tl uptake in a slow-growing bronchioloalveolar carcinoma has also been reported (*22*). Thus, attempts to correlate the above-normal ^{201}Tl uptake of lung cancers with their biologic characteristics such as cell differentiation have not produced conclusive results. In the current study, no significant difference was found between the mean ^{201}Tl T/N of bronchioloalveolar carcinomas and that of poorly differentiated adenocarcinomas. Thus, a correlation was not found between ^{201}Tl uptake and the degree of cell differentiation in adenocarcinoma of the lung, whereas FDG uptake reflected the degree of cell differentiation.

Several reasons are possible for the discordance between FDG and ^{201}Tl distributions. First, the mechanisms of accumulation of these tracers in tumors are different. FDG is transported, phosphorylated, and metabolically trapped in tumor cells as FDG-6-phosphate. The mechanisms for increased FDG-6-phosphate accumulation in many cancer cells have been shown to involve the following: increased expression of glucose transporter molecules at the tumor cell surface, increased level or activity of hexokinase, and reduced levels of glucose-6-phosphatase compared with most normal tissue (*23*). The mechanisms of ^{201}Tl uptake in tumor cells have not been clearly defined. Thallium is a potassium analog and is transported into the cell in place of potassium. This transportation might be related to Na^+,K^+-adenosinetriphosphatase (Na^+,K^+-ATPase); this hypothesis is supported by the results of an in vitro experiment showing that the active transport of thallium into malignant cells is inhibited by Na^+,K^+-pump blocker (*24*). In a clinical study, Takekawa et al. (*21*) reported that the ^{201}Tl T/N (delayed ratio) is significantly higher in Na^+,K^+-ATPase–positive adenocarcinomas than in Na^+,K^+-ATPase–negative adenocarcinomas. However, ^{201}Tl uptake into tumors is dependent on blood flow as well as on the Na^+,K^+-ATPase system (*5*). In bronchioloalveolar carcinoma, focal increased lung perfusion has been observed, and blood flow may be a possible contributing factor of ^{201}Tl uptake in bronchioloalveolar carcinoma (*25*). Several findings suggest that cell incorporation of ^{201}Tl is not directly related to cell glycolysis activity. Kawabe et al. (*26*) have observed an abnormally high uptake of ^{201}Tl and a relatively low uptake of FDG in a region of atelectasis with a collapsed alveolar structure. Slosman and Pugin (*27*) have reported that cell incorporation of ^{201}Tl differs from that of ^{3}H-deoxyglucose in vitro. On the basis of the results of comparative ^{201}Tl SPECT and FDG PET studies, Oriuchi et al. (*28*) have also shown that ^{201}Tl uptake in gliomas may be independent of increased glucose transport or metabolism.

Second, the spatial resolutions and the sensitivities are strikingly different between PET and SPECT (*29*), which may cause a great difference in image quality. Ikeda et al. (*30*) have reported that ^{201}Tl SPECT with a triple-head gamma camera revealed only 10 of 20 small lung cancers of $\leq$2 cm in diameter. In the current study, FDG PET identified 3 additional lung cancers that ^{201}Tl SPECT images did not reveal. Two of these lung cancers were moderately differentiated adenocarcinomas of $<$2 cm in diameter. In these instances, the difference in the spatial resolutions may be a possible contributing factor.

Third, the scintigraphic detectability depends not only on the size of the lesion and the degree of uptake of radiopharmaceuticals but also on the contrast between the lesion uptake and surrounding tissues (*29*). T/Ns between the lesions and the homologous contralateral normal lung are higher on average with FDG PET than with ^{201}Tl SPECT (*17*).

No significant difference was found between FDG PET and ^{201}Tl SPECT in the specificity for the differentiation of malignant and benign pulmonary nodules. FDG PET and ^{201}Tl SPECT showed false-positive results for the same 7 benign nodules (58.3%) in the patients with pulmonary nodules suspected to be lung cancer on chest CT. FDG is taken up not only by viable tumor cells but also by granulation tissue and activated macrophages (*8,10,11*). Tissue inflammation may manifest increased glycolysis, but the increase in the metabolic rate associated with inflammatory changes is usually substantially less than that of neoplastic tissue. Inflammation and malignancy generally are differentiated on the basis of SUV. An SUV threshold of 2.5 has been determined empirically to provide good sensitivity and specificity in differentiating benign from malignant lesions when patients with solitary pulmonary nodules are evaluated (*31*). However, in the current study, sarcoidosis showed

Downloaded from jnm.snmjournals.org by on March 14, 2017. For personal use only.

a markedly elevated SUV of approximately 10. Several benign diseases in the thorax have been reported to be associated with increased FDG accumulation. False-positive findings defined by an SUV of >2.5 have been reported in inflammatory and granulomatous processes such as aspergillosis, cryptococcosis, histoplasmosis, tuberculosis, Wegener's granulomatosis, and sarcoidosis (*2,12,13*). Sugawara et al. (*11*) have reported that FDG, which accumulates rapidly in sites of bacterial infection with a high target-to-background ratio, appears to be a promising infection detection agent.

^{201}Tl is also absorbed into the inflammatory lesions (*14*) and has been reported to be of value in the evaluation of disease activity (*15*). Tonami et al. (*6*) have reported that 16 of 23 benign lesions (70%) had significant ^{201}Tl uptake. No significant difference was found in the DR when benign and malignant lesions were compared. However, a significant difference in the RI was noted between benign and malignant lesions. In their study, the RIs for malignant and benign lesions were 25% ± 24% and 6% ± 14%, respectively. Similarly, Suga et al. (*7*) have reported that 39 of 58 benign lesions (67%) were revealed on early ^{201}Tl scans. Benign conditions showing early ^{201}Tl uptake include active tuberculosis, active pneumonia, organizing pneumonia, inflammatory pseudotumor, silicosis, radiation pneumonitis, atypical mycobacterial disease, aspergilloma, granuloma (*7*), and sarcoidosis (*32*). The findings of Suga et al. agree with those of Tonami et al. (*6*) in that no significant difference was found in the early or delayed uptake ratios in benign compared with malignant lesions, and the difference in the RI was statistically significant (23.3% ± 18.9% for malignant lesions and −4.3% ± 13.6% for benign lesions). However, atelectasis with collapsed alveolar structure may also show a high ^{201}Tl RI (*25,33*). In the current study, the ^{201}Tl RI for sarcoidosis was also high (42.9%), and FDG PET and ^{201}Tl SPECT showed false-positive results for the same 7 benign lesions (4 granulomas, 1 sarcoidosis, 1 inflammatory pseudotumor, and 1 aspergilloma). Thus, no significant difference was found between FDG PET and ^{201}Tl SPECT in the specificity for differentiation of malignant and benign pulmonary nodules. When interpreting FDG PET and ^{201}Tl SPECT images, caution should be exercised in patients with pulmonary nodules suspected to be lung cancer.

In the evaluation of pulmonary nodules using FDG PET and ^{201}Tl SPECT, negative FDG PET findings and positive ^{201}Tl SPECT findings were observed only for bronchioloalveolar carcinomas or a well-differentiated adenocarcinoma, but this result was not observed for other histologic types of lung cancers or benign pulmonary nodules. Thus, the findings may be specific for bronchioloalveolar carcinoma or well-differentiated adenocarcinoma, and the combination of FDG PET and ^{201}Tl SPECT may provide additional information regarding the tissue characterization of pulmonary nodules.

This study had several limitations in terms of the patient population. First, many patients with adenocarcinomas were included. Forty-four of 51 patients (86.3%) had adenocarcinomas, and only 6 of 51 patients (11.8%) had squamous cell carcinomas. This study included only surgically removed nodules. Therefore, almost all nodules in this study were located at the periphery of the lung. Adenocarcinoma is the tumor most often observed peripherally. Squamous cell carcinoma often arises in or immediately adjacent to lobar bronchi and is occasionally peripheral. Second, this study also included many bronchioloalveolar carcinomas. Eleven of 44 adenocarcinomas (25%) were bronchioloalveolar carcinomas. Recent evidence suggests that the number of cases of adenocarcinoma of the lung has increased dramatically in the last decade and that this is largely attributed to an increase in bronchioloalveolar carcinoma (*34,35*). Furthermore, this study included only resected cases. Therefore, inoperable adenocarcinomas were excluded. Bronchioloalveolar carcinoma is a well-differentiated, slow-growing tumor and is usually operable. Third, this study included only 12 patients with benign pulmonary nodules because only pulmonary nodules suspected to be lung cancer on the basis of chest CT and removed surgically were included. Therefore, few conclusions can be drawn from these data regarding the true-negative rate on FDG PET and on ^{201}Tl SPECT. In these respects, additional investigation is warranted.

CONCLUSION

In this preliminary study, no significant difference was found between FDG PET and ^{201}Tl SPECT in the specificity for the differentiation of malignant and benign pulmonary nodules. The degree of differentiation of lung adenocarcinoma correlated with FDG uptake but not with ^{201}Tl uptake. Bronchioloalveolar carcinoma, a well-differentiated, slow-growing tumor, typically was positive on ^{201}Tl SPECT but was negative on FDG PET. The combination of FDG PET and ^{201}Tl SPECT may provide additional information regarding the tissue characterization of pulmonary nodules.

ACKNOWLEDGMENTS

This work was supported by a Grant for Project Research (H00-2) from the High-Technology Center of Kanazawa Medical University, a Grant-in Aid for Cancer Research (12-4) from the Ministry of Health and Welfare, Japan, and a Grant-in Aid for Scientific Research (08670224) from the Ministry of Education, Science, and Culture, Japan.

REFERENCES

1. Mark MJ, Hazelrigg SR, Landreneau RJ, Acuft TE. Thoracoscopy for the diagnosis of the indeterminate solitary pulmonary nodule. *Ann Thorac Surg*. 1993;56:825–832.
2. Coleman RE. PET in lung cancer. *J Nucl Med*. 1999;40:814–820.
3. Prauer HW, Weber WA, Romer W, et al. Controlled prospective study of positron emission tomography using the glucose analogue [^{18}F]fluorodeoxyglucose in the evaluation of pulmonary nodules. *Br J Surg*. 1998;85:1506–1511.

Downloaded from jnm.snmjournals.org by on March 14, 2017. For personal use only.

4. Lowe VJ, Fletcher JW, Gobar L, et al. Prospective investigation of positron emission tomography in lung cancer. *J Clin Oncol*. 1998;16:1075–1084.
5. Chin BB, Zukerberg BW, Buchpiguel C, et al. Thallium-201 uptake in lung cancer. *J Nucl Med*. 1995;36:1514–1519.
6. Tonami N, Yokoyama K, Shuke N, et al. Evaluation of suspected malignant pulmonary lesions with Tl-201 single-photon emission computed tomography. *Nucl Med Commun*. 1993;14:602–610.
7. Suga K, Kume N, Orihashi N, et al. Difference in Tl-201 accumulation on single photon emission computed tomography in benign and malignant lesions. *Nucl Med Commun*. 1993;14:1071–1078.
8. Kubota R, Yamada S, Kubota K, et al. Intramural distribution of ^{18}F-fluorodeoxyglucose in vivo: high accumulation on macrophages and granulation tissues studied by microautography. *J Nucl Med*. 1992;33:1972–1980.
9. Kapucu LO, Meltzer CC, Townsend DW, et al. Fluorine-18-fluorodeoxyglucose uptake in pneumonia. *J Nucl Med*. 1998;39:1267–1269.
10. Yamada S, Kubota K, Kubota R, Ido T, Tamahashi N. High accumulation of fluorine-18-fluorodeoxyglucose in turpentine-induced inflammatory tissue. *J Nucl Med*. 1995;36:1301–1306.
11. Sugawara Y, Gutowski TD, Fisher SJ, Brown RS, Wahl RL. Uptake of positron emission tomography tracers in experimental bacterial infections: a comparative biodistribution study of radiolabeled FDG, thymidine, L-methionine, Ga-67 citrate, and I-125 HSA. *Eur J Nucl Med*. 1999;26:333–341.
12. Lewis PJ, Salama A. Uptake of fluorine-18-fluorodeoxyglucose in sarcoidosis. *J Nucl Med*. 1994;35:1647–1649.
13. Larson SM. Cancer or inflammation? A holy grail for nuclear medicine. *J Nucl Med*. 1994;35:1653–1655.
14. Ando A, Ando I, Katayama M, et al. Biodistributions of ^{201}Tl in tumor bearing animals. *Eur J Nucl Med*. 1987;12:567–572.
15. Utsunomiya K, Narabayashi I, Nishigawa H, et al. Clinical significance of thallium-201 and gallium-67 scintigraphy in pulmonary tuberculosis. *Eur J Nucl Med*. 1997;24:252–257.
16. Higashi K, Ueda Y, Seki H, et al. Fluorine-18-FDG imaging is negative in bronchioloalveolar lung carcinoma. *J Nucl Med*. 1998;39:1016–1020.
17. Higashi K, Nishikawa T, Seki H, et al. Comparison of fluorine-18-FDG PET and Tl SPECT in evaluation of lung cancer. *J Nucl Med*. 1998;39:9–15.
18. Higashi K, Ueda Y, Sakurai A, et al. Correlation of Glut-1 glucose transporter expression with F-18 FDG uptake in non-small cell carcinoma. *Eur J Nucl Med*. 2000;27:1778–1785.
19. Higashi K, Ueda Y, Yagishita M, et al. FDG PET measurement of the proliferative potential of non-small cell lung cancer. *J Nucl Med*. 2000;41:85–92.
20. Duhaylongsod FG, Lowe VJ, Patz EF, et al. Lung tumor growth correlations with glucose metabolism measured by fluoride-18 fluorodeoxyglucose positron emission tomography. *Ann Thorac Surg*. 1995;60:1348–1362.
21. Takekawa H, Itoh K, Abe S, et al. Thallium-201 uptake, histopathological differentiation and Na-K ATPase in lung adenocarcinoma. *J Nucl Med*. 1996;37:955–958.
22. Kynuya S, Takahashi S, Saito M, et al. Intense and prolonged Tl-201 accumulation in a slow growing bronchioloalveolar carcinoma. *Ann Nucl Med*. 1996;10:261–264.
23. Wahl RL. Positron emission tomography: applications in oncology. In: Murray IPC, Ell PJ, eds. *Nuclear Medicine in Clinical Diagnosis and Treatment*. vol. 2. New York, NY: Churchill Livingstone; 1994:801–820.
24. Sehwil AM, McKillop JH, Milroy R, et al. Mechanism of Tl-201 uptake in tumors. *Eur J Nucl Med*. 1989;15:376–379.
25. Sarlin RF, Schillaci RF, Georges TN, et al. Focal increased lung perfusion and intra pulmonary veno-arterial shunting in bronchiolo-alveolar carcinoma. *Am J Med*. 1980;68:618–623.
26. Kawabe J, Okamura T, Shakudo M, et al. Thallium and FDG uptake by atelectasis with bronchogenic carcinoma. *Ann Nucl Med*. 1999;13:273–276.
27. Slosman DO, Pugin J. Lack of correlation between tritiated deoxyglucose, thallium-201 and technetium-99m-MIBI cell incorporation under various cell stresses. *J Nucl Med*. 1994;35:120–126.
28. Oriuchi N, Tomiyama K, Inoue T, et al. Independent thallium-201 accumulation and fluorine-18-fluorodeoxyglucose metabolism in glioma. *J Nucl Med*. 1996;37:457–462.
29. Martin WH, Delbeke D, Patton JA, Sandler MP. Detection of malignancies with SPECT versus PET, with 2-[fluorine-18]fluoro-2-deoxy-D-glucose. *Radiology*. 1996;198:225–231.
30. Ikeda E, Taki J, Kinuya S, Nakajima K, Tonami N. Thallium-201 SPECT with triple-headed gamma camera for differential diagnosis of small pulmonary nodular lesion 20 mm in diameter or smaller. *Ann Nucl Med*. 2000;14:91–95.
31. Patz EF, Lowe VJ, Hoffmann JM, et al. Focal pulmonary abnormalities: evaluation with fluorine-18 fluorodeoxyglucose PET scanning. *Radiology*. 1993;188:487–490.
32. Schraml FV, Turton DB, Bakalar RS, Silverman ED. Persistent asymmetric pulmonary Tl-201 uptake in type III sarcoidosis. *Clin Nucl Med*. 1995;20:1093–1094.
33. Lee JD, Lee BH, Kim SK, Chung KY, Shin DH, Park CY. Increased thallium-201 uptake in collapsed lung, a pitfall in scintigraphic evaluation of central bronchogenic carcinoma. *J Nucl Med*. 1994;35:1125–1128.
34. Barsky S, Cameron R, Osann KE, Tomita D, Holmes C. Rising incidence of bronchioloalveolar lung carcinoma and its unique clinicopathologic features. *Cancer*. 1994;73:1163–1170.
35. Auerbach O, Garfinkel L. The changing pattern of lung carcinoma. *Cancer*. 1991;68:1973–1977.

SOCIETY OF NUCLEAR MEDICINE

Downloaded from jnm.snmjournals.org by on March 14, 2017. For personal use only.

JNM The Journal of NUCLEAR MEDICINE

Comparison of [^{18}F]FDG PET and ^{201}Tl SPECT in Evaluation of Pulmonary Nodules

Kotaro Higashi, Yoshimichi Ueda, Tsutomu Sakuma, Hiroyasu Seki, Manabu Oguchi, Mitsuru Taniguchi, Suzuka Taki, Hisao Tonami, Shogo Katsuda and Itaru Yamamoto

J Nucl Med. 2001;42:1489-1496.

This article and updated information are available at:
http://jnm.snmjournals.org/content/42/10/1489

Information about reproducing figures, tables, or other portions of this article can be found online at:
http://jnm.snmjournals.org/site/misc/permission.xhtml

Information about subscriptions to JNM can be found at:
http://jnm.snmjournals.org/site/subscriptions/online.xhtml

The Journal of Nuclear Medicine is published monthly.
SNMMI | Society of Nuclear Medicine and Molecular Imaging
1850 Samuel Morse Drive, Reston, VA 20190.
(Print ISSN: 0161-5505, Online ISSN: 2159-662X)

© Copyright 2001 SNMMI; all rights reserved.

SNMMI SOCIETY OF NUCLEAR MEDICINE AND MOLECULAR IMAGING